In-situ crosslinking of polysiloxane electrolyte within Al_2O_3@SiNWs for quasi-solid-state micro-supercapacitors

Mathieu Deschanels, Marc Dietrich, Pascal Gentile, Fannie Alloin, Cristina Iojoiu, Saïd Sadki

In-situ crosslinking of polysiloxane electrolyte within Al_2O_3@SiNWs for quasi-solid-state micro-supercapacitors

Mathieu Deschanels,[a,c] Marc Dietrich,[a,b] Pascal Gentile,[b] Fannie Alloin,[c] Cristina iojoiu[c] and Saïd Sadki[a]*

[a] Prof. S. Sadki*, M. Dietrich, Dr. M. Deschanels
University Grenoble Alpes, CEA, CNRS, Grenoble INP, IRIG-SyMMES UMR 5819, F-38000 Grenoble, France
E-mail : said.sadki@cea.fr
[b] P. Gentile, M. Dietrich
University Grenoble Alpes, CEA, Grenoble INP, IRIG-Pheliqs, F-38000 Grenoble, France
[c] M. Deschanels, C. Iojoiu, F. Alloin,
Univ. Grenoble Alpes, Univ. Savoie Mont Blanc, CNRS, Grenoble INP, LEPMI, 38000 Grenoble, France

Abstract

Developing flexible solid-state micro-supercapacitors with large potential window is crucial for many technologies. The present study focuses on the synthesis and elaboration of quasi-solid-state (QSS) electrolytes with an electrochemical stability greater than 3.0 V based on functionalized polysiloxane. Their electrochemical behavior was studied with silicon nanowires electrodes. The polysiloxane was functionalized with both ammonium and cross-linkable functions. The nanostructured electrodes were impregnated with a mixture of ionic liquid and functionalized polysiloxane. The crosslinking of the polymer electrolyte was then performed by thermal curing directly within the nanostructured electrodes. The quasi-solid system exhibits very high stability upon galvanostatic cycling i.e. during 100 000 cycles with a cell potential of 3.0 V only a capacitance loss of 2.10^{-5} % per cycle was registered. The performance of this QSS with safe electrolyte is remarkable.

Keywords: in-situ crosslinking polysiloxane, silicon nanowires, micro-supercapacitors

Graphical abstract

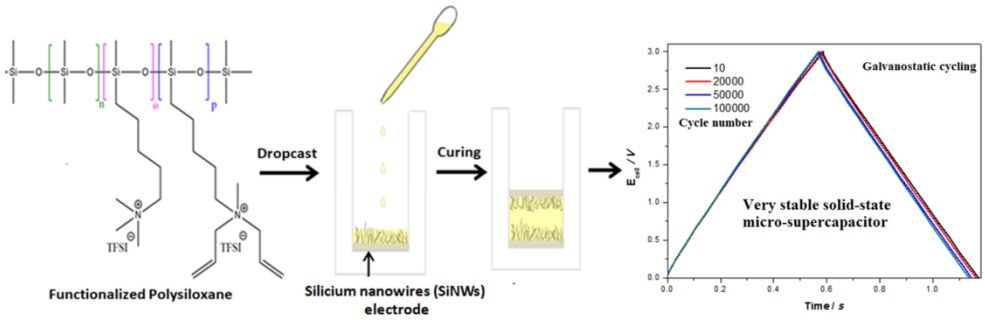

1. Introduction

Miniaturization of electronics is responsible for the development of many technology over the past decades [1]. In order to further develop micro-electronics systems, embedded micro energy storage system are required [2]. Moreover the demand in flexible and portable electronics is greatly increasing nowadays.[3,4] Those systems are advantageously used in many different fields such as textile industry,[4] biomedical devices[6] and wireless sensor networks[7] for example. Two types of devices are especially studied to meet up with the requirements of those technologies. Li-ion micro-batteries may be used because of their superior energy density, however their life time (numbers of cycles before capacity fades) is usually too low and their use would require costly and complicate maintenance especially in miniaturized system for which internal accessibility to replace part of the device may not be possible. The micro-supercapacitors (MSCs) show greater lifetime than the batteries and are particularly adapted for stop and go applications thanks to their high-power density. For those reasons, great interest was showed towards miniaturizing supercapacitors (SCs) and integrating them towards on chip or flexible substrates.[7–9]

Silicon nanowires electrodes (SiNWs) were studied as potential electrodes for MSCs especially for their use for on-chip micro-supercapacitors.[10–14] Many of the studies of SiNWs were done in liquid electrolytes.[13–15] However for MSCs applications, solid electrolyte would highly simplify the fabrication and packaging process. Moreover, solid electrolyte are also known to allow great safety.[16,17] QSS-MSCs using silicon nanowires based electrodes were mostly studied with poly(vinyl alcohol) (PVA) aqueous based gel electrolyte.[10,18,19] The first issue of this polymer electrolytes is a low potential window (usually the cell potential is between 0.8 and 2.0 V) due to water electrochemical stability. The second issue concerns the evaporation of the solvent with time that is rarely mentioned and which causes an important increase of the internal resistance of the device with time.[20] In order to avoid the issues linked to aqueous based gel polymer electrolyte, a study of J. Le Bideau *et al.* demonstrated the possibility to use ionic liquid based gel polymer electrolyte with SiNWs electrodes.[17] The authors developed a quasi-solid state electrolyte by a sol-gel process using silane precursors in ionic liquid (ethylmethyl imidazolium bis(trifluoromethanesulfonyl)imide). The results obtained were very promising demonstrating a cell potential of 4.0 V which confirms the importance of developing polymer electrolytes for applications with SiNWs electrodes.[17]

The glass transition temperature (T_g) is considered as one of the main parameter driving the viscosity as well as the conductivity of polymer electrolytes.[21] Polysiloxane is polymer with very low T_g that are usually amorphous and exhibit low viscosity at room temperature. They are considered as the class of the most flexible polymers.[22] Those polymers have also good chemical and electrochemical stabilities with high resistance to temperature.[23–25] In addition to those promising properties, their physical state at room temperature could allow to directly fill electrodes with the polymer electrolyte solventless within 3 D nanostructured electrodes.

Indeed, such polymers are very hydrophobic and need to be functionalised with ionic functions to ensure ionic conductivity and compatibility towards polar compounds. The most common functionalisation of polysiloxane is the hydrosilylation reaction. Many different types of chemical moieties of interest for electrochemical storage applications such as carbonate,[26,27] PEO,[27,29] imidazolium,[24,27] ammonium[29,30] were grafted and studied for Li-ion or lithium polymer batteries[31–35] and dye-sensitized solar cells[36–39].

In this study, functionalized polysiloxane was, as electrolyte for MSCs, for the first time used. A bi-functionalised polysiloxane, i.e. with two ammonium side chain groups, trimethylammonium (TMA) and diallylmethylammonium (DMA) was synthesized. The objective was to bring ionic conductive properties to the polymer and to facilitate the compatibility of the lipophilic polymer with an ionic liquid (IL) such as propylmethylimidazolium bis(trifluoromethanesulfonyl)imide (PMImTFSI). The DMA moiety has the particularity to be a crosslinkable function and allows to develop, in combination with IL, a QSS membrane through thermal crosslinking process.[40] The polymer electrolyte was developed with a very versatile synthesis method and its properties such as ionic conductivity, T_g and electrochemical stability could be adapted by changing the pendants, functionalization degree or/and anion nature.
SiNWs coated with a 3 nm alumina layer (Al_2O_3@SiNWs) were used as electrodes for the study and were previously developed in our laboratory.[41] The coating with alumina was previously studied and discussed to enable better stability of the SiNWs electrodes [42]. Formulation containing IL and the functionalized polysiloxane were prepared and the crosslinking of the polymer was done after an impregnation of nanostructured silicon electrodes already setup as a full cell device. The quasi-solid-state device was cycled for 100 000 times and showed great stability, with a capacitance loss of 2.10^{-5} % per cycle. The cell was cycled for different charging time and the capacitance remained stable for charging time higher than 270 ms.

2. Experimental

5-bromo-1-pentene (purity >95% GC grade), LiTFSI (purity > 98%), and trimethylamine (2 M in THF) were bought from TCI. Platinum(0)-1,3-divinyl-1,1,3,3-tetramethyldisiloxane complex solution (2.1-2.4% in xylene) was bought from ABCR. (25-35% methylhydrosiloxane)-dimethylsiloxane copolymer, trimethylsiloxane terminated with a molecular weight of 1900-2000 g/mol was bought from Gelest. Diallylmethylamine (purity 98%) was bought from Thermo Scientific™. The Amberlite 900 Cl^- ionic exchange resin was bought from Sigma Aldrich. The 1-Propyl-3-methylimidazolium bis(trifluoromethanesulfonyl)imide was synthesized. The product being commercial and the process well known, the synthesis process and the materials used for its synthesis will be described in SI.

2.1 Synthesis process

2.1.1 - Synthesis of BrPDMS

The polydimethylsiloxane bearing bromopentane fonctions were synthesized by hydrosilylation reaction following a previously reported procedure. Briefly, 4g HPDMS are dried in an argon flush during 15 minutes before adding 50 mL of dried toluene, then the solution was heated at 60°C. 0.67 mL of Platinum(0)-1,3-divinyl-1,1,3,3-tetramethyldisiloxane complex solution (2.1-2.4% in xylene) is then added slowly. 1.2 equivalents vs the Si-H functionality of 1-5-bromopentene was added to the above solution drop-wise under constant stirring. After 3 hours of reaction at 80°C in reflux, ^{1}H NMR confirms the end of the synthesis. After purification, the yield for the synthesis is equal to 96 %.

^{1}H NMR (400 MHz, acetone-D6, δ): 3.55-3.45 ppm (-CH_2-Br), 1.97-1.83 ppm (-**CH_2**-CH_2-Br), 1.61-1.40 ppm (Si-CH_2-**CH_2**-**CH_2**-CH_2-Br) 0.7-0.55 ppm (-CH_2-Si), 0.29-0.06 ppm (CH_3-Si)

2.1.2 - Synthesis of $DMA_{65}Br_{35}$PDMS

The incorporation of the ammonium function was performed by nucleophilic substitution. In a typical procedure 4 g of BrPDMS is introduced in a flask covered with aluminum to avoid degradation of the tertiary amine with light. A mixture of THF and absolute ethanol was added in other to solubilize both the BrPDMS and the resulting PDMS containing ammonium side chains. To this mixture, 3 equivalents of methyldiallylamine vs bromine moieties were added. The solution is heated at 60°C for around 2 weeks. After solvent evaporation, the polymer was purified by a dialysis process. The polymer is then dried again in rotary evaporator before the next reaction step. The synthesis yield is equal to 90%.

^{1}H NMR (400 MHz, DMSO-D6, δ) : 6.20-5.90 ppm (-**CH**=) 5.75-5.55 ppm (=**CH_2**) 4.14-3.86 ppm (=CH-**CH_2**-N^+) 3.53-3.35 ppm (-**CH_2**-Br) 3.28-3.09 ppm (-CH_2-**CH_2**-N^+) 3.08-2.89 ppm (**CH_3**-N^+), 1.86-1.61 ppm (Br-CH_2-**CH_2**-) + (N^+-CH_2-**CH_2**), 1.46-1.18 ppm (-**CH_2**-**CH_2**-CH_2-Si) 0.6-0.37 ppm (-**CH_2**-Si), 0.17-0.00 ppm (**CH_3**-Si)

2.1.3 - Synthesis of $DMA_{65}TMA_{35}$(Br)PDMS

Around 4 g of $DMA_{65}Br_{35}$PDMS are dissolved in 20 mL of absolute ethanol in a flask under argon covered with aluminum. 5 equivalents of trimethylamine are added using a 2 mol.L^{-1} trimethylamine in THF solution. The flask is heated and stirred at 60 °C for 24 h. The yield for this step is equal to 98 %.

^{1}H NMR (400 MHz, DMSO-D6, δ) : 6.2-5.9 ppm (-**CH**=) 5.75-5.55 ppm (=**CH_2**) 4.14-3.86 ppm (=CH-**CH_2**-N^+) 3.31-3.09 (-**CH_2**-N^+-$(CH_3)_3$) + (-CH_2-**CH_2**-N^+) 3.08-2.89 (**CH_3**-N^+) + ((**$(CH_3)_3$**-N^+), 1.86-1.61 ppm ($(CH_3)_3$-N^+-CH_2-**CH_2**-) + (N^+-CH_2-**CH_2**), 1.46-1.18 ppm (-**CH_2**-**CH_2**-CH_2-Si) 0.6-0.37 ppm (-**CH_2**-Si), 0.17-0.00 ppm (**CH_3**-Si)

2.1.4 - Synthesis of $DMA_{65}TMA_{35}$(TFSI)PDMS

Anion exchange was performed on an anionic exchange resin IRA 900 Cl^-. In a first step, the Cl^- from the resin are changed into $TFSI^-$ by mixing the resin with around 300 mL of an aqueous solution containing 110 g of LiTFSI (10 times more $TFSI^-$ with regards to Cl^- on the resin). Then the resin is placed in a column and washed with water until the washing water conductivity reach around 10 µS cm^{-1}. The column is then washed one last time with acetonitrile. 4 g of $DMA_{65}TMA_{35}$(Br)PDMS in acetonitrile is slowly passing through the column 8 times, with 5 times more $TFSI^-$ with regard to Br^- anion. After acetonitrile removed, the polymer is purified by dialysis and dried. The yield for this step is equal to 84 %.^{1}H NMR is given in fig. SI 2. Anion exchange was confirmed by the presence of $TFSI^-$ showed by fluorine NMR coupled with the absence of Li^+ on ^{7}Li NMR. In addition, no precipitation of AgBr was observed after the addition of $AgNO_3$, proving the absence of Br^- into the polymer.

2.2 Preparation of the Al_2O_3@SiNWs

The electrodes that were used to study the polymer electrolyte in device conditions are alumina coated silicon nanowires electrodes. The preparation of those electrodes is described in our previous work.[39] Briefly, silicon nanowires growth is done on highly n-doped silicon wafers by a chemical vapor deposition process allowing the growth of around 50 µm length n-doped nanowires. Then a nanometric alumina layer (3 nm) is deposited by an atomic layer deposition process. The electrodes surface is 1 cm².

2.3 Preparation of the UV crosslinked membrane for conductivity measurements

To prepare the membranes for conductivity measurements, several solutions were prepared and drop casted in Teflon petri dish. The solution consisted of $DMA_{65}TMA_{35}$(TFSI)PDMS, Darocur 1173 and PMImTFSI for the one containing ionic liquid. The molar ratio between diallylammonium moieties (crosslinking pendant group) and the thermal initiator was kept to 6. For membrane containing PMImTFSI, molar equivalences of 0.25, 0.5, 0.75 between ionic liquid and ammonium moieties in the polymer (trimethylammonium + diallylmethylammonium) were used. This corresponds respectively to 12 and 29 wt.% of ionic liquid in the membrane.

Around 300 mg of solution is prepared every time and drop casted in Teflon petri dish (r = 2 cm). The petri dish is then put under 254 nm UV lamps for 5 minutes. The membrane is then dried under vacuum at 40°C in a dryer, the pressure is decreased gradually: it starts 0.7 bars and was decreased by 0.2 bar every 15 minutes until reaching the maximum vacuum for the pump at 10^{-3} mbar. Then the temperature was increased at 60°C and keep overnight under vacuum. Then the membrane drying process is finished in a büchi

cell at 80 °C under vacuum (10^{-3} mbar) for 24 h before the membrane is introduced in glovebox. The membranes after drying are around 100 µm thick.

2.4 Preparation of the full cell device

First an Al_2O_3@SiNWs electrode is deposited on the bottom of the mold. Then a solution containing 75 wt% of $DMA_{65}TMA_{35}$(TFSI)PDMS, 22 wt% of PMImTFSI and 3 wt% of benzoyl peroxide is prepared, in order to obtain the electrolyte named $DMA_{65}TMA_{35}$(TFSI)PDMS + 0.5 IL. To facilitate the solubilization of benzoyl peroxide, few drops of acetone are added to the mixture. The solution is then stirred at 40 °C during around 10 minutes to help the solubilization of benzoyl peroxide and evaporate most of the acetone in the mixture. Then this solution is slowly deposited on the electrode until the full surface is wetted (which corresponds to around 4 drops and 40 mg). The second electrode is then added and a very small pressure is applied on the entire electrode ensuring that the second electrode is fully wetted. The mold is then placed in a dryer which is put under very progressive vacuum to remove potential residual acetone traces. Then the mold is heated vacuum less at 80 °C for 72 h in the dryer. After that time, the mold is removed to grab the device. The wafer side of the electrodes is polished with diamond paste to remove the excess polymer on the current collector side and allows good electric contact. Before electrochemical study, the device is dried under vacuum at 60 °C over night before being used inside the glovebox.

2.5 Electrochemical characterization

The electrochemical measurements were performed with a potentiostat/galvanostat (VMP3, Biologic, France).

2.5.1 - Potential window determination

The three electrodes measurement was done on a home-made cell. The working electrode is platinum electrode with a disk like flat surface with radium of 1.5 mm. The counter electrode is a platinum coil and the reference used a silver wire. The electrodes are tightened together on the insulating Teflon part of the working electrode and the interelectrode distance is minimized to around 2 mm. Prior to experiments, the silver reference was calibrated with ferrocenium/ferrocene couple (-0.21 V vs Fc^+/Fc) as an internal reference in the polymer electrolyte. This was used to express the potential towards the Fc^+/Fc couple. The experiments are done in glove box. The electrodes were cleaned and polished before each experiment. Linear sweep voltammetry with a scan rate of 5 mV s^{-1} was done to determine the potential window of the polymer electrolyte.

2.5.2 - Cyclic voltammetry and galvanostatic measurements

The developed full cell was studied electrochemically by cyclic voltammetry and galvanostatic measurements in symmetric system with 2 electrodes configuration in ECC-Std test cell FED9015 from EL-CELL. The pressure applied by the external cell on the two electrodes device is around 12 N cm^{-2}.

For the stability measurement, 100 000 galvanostatic cycles were performed with a current density of 0.1 mA cm^{-2}. The cell was charged up to 3 V.

Capacitance (C) was determined from galvanostatic cycling with the equation (1):

$$C = \frac{I\Delta t}{\Delta U.\,S} \tag{1}$$

Where I corresponds to the applied discharging current, Δt to the time of discharge, ΔU to the maximum cell potential and S to the geometrical surface of the device.

Coulombic efficiency (CE) was determined with the equation (2):

$$CE = \frac{t_d}{t_c}.100 \qquad in\ pourcentage \tag{2}$$

Where t_d corresponds to the time of discharge and t_c to the time of charge.

About studying the effect of fast charging on the capacitance of the devices, cyclic voltammetry was performed between 0 and 3 V for scan rates ranging from 1 to 10 V s^{-1}

The capacitance (C) was determined with equation (3):

$$C = \frac{\int IdU}{v.\,S.\,\Delta U} \tag{3}$$

With v the scan rate applied.

2.5.3 - Electrochemical impedance spectroscopy

Ionic conductivity was measured by electrochemical impedance spectroscopy, using an HP 4192A impedance analyzer in the frequency range 5 Hz–13 MHz. The membrane was sandwiched between two stainless steel blocking electrodes. Measurements were done between -20 and 90 °C every 10 °C.

2.6 Physicochemical characterization

Glass transition temperature of the membranes were recorded using differential scanning calorimeter (DSC 1-Mettler-Toledo). Each sample was scanned with a temperature ramp of 10 °C min^{-1} with a temperature range between -120 and 100 °C under nitrogen atmosphere.

^{1}H NMR and ^{13}F NMR spectra were run on Bruker Advance 400 spectrometer and performed in acetone D-6 or DMSO D-6

Full cell and silicium nanowires electrodes were examined by scanning electron microscopy (SEM) (Zeiss Ultra 55, Zeiss, Oberkochen, Germany)

3. Results and Discussion

3.1 Chemical synthesis of $DMA_{65}TMA_{35}$(TFSI)PDMS :

The bi-functionalization polysiloxane was obtained by modification of commercial copolymer (25-35% Methylhydrosiloxane)-Dimethylsiloxane copolymer, trimethyl siloxane terminated (HPDMS) from Gelest, with a 65/35 % ratio between dimethylsiloxane and methylhydrosiloxane moieties and terminated in trimethylsiloxane. The overall synthesis process is described figure 1.

The first step of the chemical modification concerned the addition of 1-5-bromopentene through a hydrosilylation reaction (1). This reaction gave a high yield of 96 %. In a second step the quaternization reaction with diallylmethylamine was performed. To optimize the polymer functionalization and crosslinking degree, two degree of functionalisation were performed i.e. 35% and 65 % of the bromide functions were transformed in DMA, the unreacted brominated moieties were then quaternarised with trimethylamine. ^{1}H NMR of the 35 % functionalized polymer can be seen in fig. SI 3. The quaternization reactions with methyldiallylamine are longer than those with trialkyl amines (even with an excess of 3 equivalents of the methyldiallylamine) around 2 weeks are needed to reach the desired functionalization of 65 % while the reaction with trimethylamine, in the second quaternization step, is finished after around 24 h.
In the last synthesis step, bromide anion (Br^-) was exchanged with bis(trifluoromethanesulfonyl)imide anion ($TFSI^-$). This exchange process is necessary because bromide anion is not adapted for the application for several reasons: (i) the electrochemical stability, the bromide will be oxidized at low anodic potential and thus affecting the electrochemical stability of the electrolyte, (ii) the localized anion charge on bromide will create strong ions pairing inducing an increase of the T_g and T_m and very poor conductivity, especially at low temperature. The $TFSI^-$ has the advantage of a largely delocalized ion charge and high flexibility. The study of Bocharova *et al.* on polysiloxane electrolytes proved that by changing the bromide to $TFSI^-$, a strong decrease of the polymer T_g was obtained i.e. from 3 to -40 °C.[20] To perform this anion exchange, an anion exchange resin (IRA 900 Cl^-) was used. The obtained copolymer will be referred as DMA_xTMA_y(TFSI)PDMS where x and y are the degrees of functionalization with DMA and TMA respectively. Membranes from both PDMS modifications were synthetised however those obtained from 35 % DMA ($DMA_{35}TMA_{65}$(TFSI)PDMS) were too soft for the application therefore for the next characterizations only those with 65% of DMA ($DMA_{65}TMA_{35}$(TFSI)PDMS) will be discussed.

3.2 Electrochemical characterization: $DMA_{65}TMA_{35}$(TFSI)PDMS

The $DMA_{65}TMA_{35}$(TFSI)PDMS electrochemical stability was studied in a three-electrodes setup by linear voltammetry (fig. 2 a).
One should note that determining the potential window of an electrolyte is quite arbitrary and depends on the conditions applied.[43] In this study, we decided to use a platinum (Pt) working electrode which was reported to be the electrode giving the lower potential window because of the catalytic properties of this material, to work with a very small distance between electrodes to lower the impact of electrolyte resistivity on the measurement and to take very low cut-off of current density (0.01 $mA.cm^{-2}$) to avoid overestimating the electrochemical stability of the polymer.
The electrochemical stability of $DMA_{65}TMA_{35}$(TFSI)PDMS is larger than 3.00 V**.** A reduction is observed at -1.85 V *vs* Fc^+/Fc which could be related to either ammonium cations or $TFSI^-$ anions reduction. Indeed, the reduction of ammoniums such as tetraethylammonium iodide was observed in propylene carbonate at -2.10 V vs Fc^+/Fc[44]. $TFSI^-$ reduction was observed at -2.00 V *vs* Fc^+/Fc in N-propyl-pyrrolidinium TFSI ionic liquid[45].
At anodic potentials, the degradation is observed around 1.60 V. Oxidation of $TFSI^-$ anions were previously observed in propylene carbonate using glassy carbon working electrode for a potential of 5.40 V vs Li^+/Li corresponding to around 1.80 V vs Fc^+/Fc[46]. This observation was then confirmed by ab initio calculation expecting an oxidation of $TFSI^-$ anions at 5.30 V vs Li^+/Li.[47] Another possible degradation could come from the oxidation of the ammonium chain which was observed between 1.60 V and 2.10 V vs Fc^+/Fc for different ammonium based ionic liquid with different alkyl chains lengths using Pt working electrode. A similar oxidation peak was also reported for some polysiloxane based electrolytes, but its origin was not assigned.[32–34] However, a theoretical study on siloxane showed the possible Si-O bond disruption and proposed several mechanisms to it at 4 V *vs* Li^+/Li.[24] Nevertheless, polysiloxanes are considered extremely stable in oxidation and the oxidation of the ammonium chain seems more likely.

The conductivities were studied with crosslinked membranes prepared through UV irradiation process of different blends of $DMA_{65}TMA_{35}$(TFSI)PDMS and PMImTFSI. The resulting membranes were sandwiched between stainless steel electrodes and their resistances were measured by electrochemical impedance spectroscopy (EIS) in the range of temperature -20°C to 90 °C. The results are showed in fig. 2 b and conductivity values at 0, 20, 90°C and T_g of the different membranes are summarized in table 1.
The addition of PMImTFSI induces an increase of ionic concentration and a decrease of T_g of the $DMA_{65}TMA_{35}$(TFSI)PDMS. For the T_g, a significant decrease of 20°C is observed with the addition of 0.25 molar equivalent of IL. By further increasing the IL amount, the T_g decreases in a slower way and the membrane with 0.75 molar equivalent of IL with regards to ammonium moieties in the polymer becomes sticky. As concerning the conductivity, a continuous increase is observed. At 90°C, a factor 42 is found between the conductivity of DMA_{65}+0.75 IL and DMA_{65}. This factor is greatly increased to 1650 at 0 °C. For full device study, the $DMA_{65}TMA_{35}$(TFSI)PDMS+0.5 IL membrane was chosen, giving the best compromise between ionic conductivity and mechanical properties.

3.3 Electrochemical study in full cell

In order to determine the stability of the polymer electrolyte, a cell was developed using Al_2O_3@SiNWs electrodes which were shown to be very stable for supercapacitors applications[41]. A mold was used to put the first electrode, and a solution containing ionic liquid, benzoyl peroxyde as thermal initiator and $DMA_{65}TMA_{35}$(TFSI)PDMS + IL was drop casted on the electrode as can be seen on scheme 1 (step I). The second electrode was added on top (step II) and the crosslinking was done by heating directly the full cell to get proper interface between the polymer and the nanostructured electrodes (step III).

Symmetric cell was studied with galvanostatic cycling for 100 000 cycles. The current density applied was 0.1 $mA.cm^{-2}$ corresponding to charging time of around 0.57 second. The cell was charged up to 3.0 V. Figure 3a shows the galvanostatic measurement made at 10, 20 000, 50 000 and 100 000 cycles. The galvanostatic cycling shows capacitive signature with a well-defined triangle shape, electrochemical characteristic of pure capacitive storage. The cycling appears stable upon 100 000 cycles. A capacitance of 19.6

$\mu F.cm^{-2}$ is determined which is lower to the 30 $\mu F.cm^{-2}$ obtained for this system with pure ionic liquids at the same charging rate.[13] Nevertheless the capacitance after 100 000 cycles was still 19.2 $\mu F.cm^{-2}$ corresponding to a capacitance loss of 2.10^{-5} % per cycle. The coulombic efficiency stays pretty high upon cycling and tends to increase from 92.2 % in first cycle to 99.3 % in last cycle. The lower coulombic efficiency observed at the beginning could be explained by small traces of solvents such as acetone, ethanol or water used during the synthesis or presence as few ppm in the glovebox respectively that could have stayed trapped in the membrane. The figure 3c is a zoom of the figure 3a which shows the evolution of the ohmic drop after cycling. The ohmic drop at the beginning of the cycling is around 40 mV and slowly increase upon cycling reaching around 50 mV after 100 000 cycles. Even though the coulombic efficiency is not 100 %, the degradation that could occur upon cycling does not seem to affect either the resistivity of the device since the ohmic drop change is negligible or the capacitance since it remained stable even after 100 000 cycles. The figure 3d shows the Nyquist plot before and after cycling the device. A slight increase of the electrolyte resistance is observed. The $R_{electrolyte}$ is found to be 230 Ω before cycling and 270 Ω after, which may be due to a weak increase of the cross-linking density of the membrane with time. The increase is small as what was observed on the increase of the ohmic drop. Overall the prepared membrane is stable upon cycling with a cell potential of 3.0 V.

The effect of charging time was then studied on the full cell to verify if the full cell using polymer electrolyte would allow high charging rate. This property was already observed with those electrode materials in organic electrolyte, ionic liquid and ionogel.[14,15,17] Cyclic voltammetry and galvanostatic measurements were performed at room temperature for respectively different scan rates and current densities to determine the impact of the charging and discharging time on the capacitance of the device. Cyclic voltammetry was performed at 1, 2, 5 and 10 $V.s^{-1}$ and the results are shown fig. 4 a. The voltammogram, at every scan rate, shows rectangular shape characteristic of capacitive behavior. Almost no ohmic drop can be seen from the voltammogram and the capacitance remains stable upon increasing the scan rate with a capacitance of 19.6 $\mu F.cm^{-2}$ at 1 $V.s^{-1}$ against 18.1 $\mu F.cm^{-2}$ at 10 $V.s^{-1}$ as can be seen in fig. 4c. Galvanostatic measurements were also performed and the results are shown fig. 4b. For the lowest current density applied (0.02 $mA.cm^{-2}$) corresponding to a charging time of 3.1 s, the capacitance of the device is 19.7 $\mu F.cm^{-2}$. This value slowly decreases up to a charging time of 270 ms where the capacitance is 18.2 $\mu F.cm^{-2}$. Then increasing the charging time is strongly affecting the capacitance which fades to 14.5 $\mu F.cm^{-2}$ for a charging time of 45 ms as can be seen on fig. 4c, representing the capacitance for different charging times for cyclic voltammetry and galvanostatic measurements. It seems that for charging time lower than 270 ms, the ohmic drop associated with the internal resistance of the device limits the recovered capacitance. A charging time of 270 ms is characteristic for electronic double layer capacitor as can be seen in fig. SI 6. Interesting high charging time ability were obtained with the use of our solid-state device which was very promising for the use of such solid electrolytes.

3.4 SEM images of the full cell

One should note that before using the method of preparation of the device (in-situ crosslinking), a cell using the same electrodes was developed by preparing the membrane in a Teflon petri dish, then cutting it the right size and pressing the prepared membrane between the two electrodes. The capacitance of that device was lower (8.2 $\mu F.cm^{-2}$) (fig. SI 5 b). Scanning electron microscopy (SEM) images were performed on this cell and showed that the nanowires on the electrodes were flattened potentially explaining why the capacitance was decreased (fig. SI 5 c and d).

The SEM images of the cell device obtained by *in-situ* electrolyte crosslinking as well as of Al_2O_3@SiNWs electrode alone were also performed and represented in figure 5.

The nanowires Al_2O_3@SiNWs are distinct with lengths of around 50 µm thanks to the chemical vapor deposition process. The image the full cell device, the device was cleaved first in half to get a sideview of the cell. The good affinity between the polymer electrolyte and the nanowires can be advantageously noticed. The cell showed good mechanical properties with a strong binding between the polymer and the nanowires that allowed to cleave the full cell without damaging it.

Colors were added post-imaging to the picture so one can have a better insight of the different device parts. The yellow part represents the silicon wafer, current collectors on top and bottom of the cell. The green part shows the Al_2O_3@SiNWs coated with the polymer electrolyte. Lastly, the blue part represents the polymer electrolyte separating the two electrodes. The electrolyte appears homogeneous with a thickness of around 70 µm. The silicon nanowires were not harmed during the crosslinking process and kept their shape and length of around 50 µm. Polymer electrolyte seems to be observed up to the base of the wafer, which means the electrolyte impregnates in deep the electrode porosity and proves a good affinity between the developed polymer electrolyte and the Al_2O_3@SiNWs as well as a well-adapted viscosity of electrolytes. Moreover, polysiloxane electrolyte membrane of about 70 µm measured. The thickness of the membrane was acceptable but could be reduced, which could decrease significantly the internal resistance of the cell, and then increase the cell performance. This image confirmed the benefit of this in-situ crosslinking process since the nanowires kept their good morphology and the polymer electrolyte was homogenously added in the cell, contrary to the process when crosslinked membrane is sandwiched under pressure between the two electrodes.

4. Conclusion

In this study, a new process to functionalize polysiloxane bearing hydrosiloxane pendant was studied. The polymer was modified via hydrosililation and quaternization reactions. The developed functionalization is very versatile. The properties of such as conductivity, T_g and electrochemical potential window of this polymer electrolyte could be adapted by changing the chain pendant, the functionalization degree and the anion nature. The new polysiloxane electrolytes presented in this work was synthesized in order to be used in presence of silicon nanowires electrode for a QSS MSC application. The polysiloxane ($MDA_{65}TMA_{35}$(TFSI)PDMS) was mixed with IL (PMImTFSI) to boost its ionic conductivity. Even for low quantity of IL (22 wt%), conductivity was greatly enhanced with a factor 160 at room temperature. The in-situ thermal crosslinking of this polymer was done solventless and directly within the nanostructured electrodes. The whole device was studied and showed excellent stability upon 100 000 cycles with 3.0 V potential window. The device retained its capacitance for charging time as low as 245 ms. The performances observed were close to the one observed with such electrodes in liquid electrolytes while having the advantages of a solid-state device. The full cell was observed by SEM and showed a homogeneous system, crackless, with polymer electrolyte filling up to the base of the silicon wafer. The electrolyte thickness of around 70 µm was enough for the system to be used without separator and can be easily reduce.

Funding

This work was supported by the Research National Agency and the ECOPE project (19-ASTR-0026-01) driving this work, the Agence Innovation Défense (AID) from the DGA, ministère de la défense, and the Commisariat à l'Energie Atomique et aux Energies Alternatives (CEA) from Grenoble

References

[1] V. Saripalli; G. Sun; A. Mishra; Y. Xie; S. Datta; V. Narayanan, IEEE Trans. Emerg. Sel. Topics Circuits Syst. **2011**, 1, 109–119
[2] C. Lethien, J. Le Bideau, T. Brousse, Energ Environ Sci., **2019**, 12, 96.
[3] Z. Zhao, K. Xia, Y. Hou, Q. Zhang, Z. Ye, J. Lu, *Chem. Soc. Rev.* **2021**, *50*, 12702–12743.
[4] Y. Wang, X. Wu, Y. Han, T. Li, *Journal of Energy Storage* **2021**, *42*, 103053.
[5] B. S. Shim, W. Chen, C. Doty, C. Xu, N. A. Kotov, *Nano Lett.* **2008**, *8*, 4151–4157.
[6] D.-C.-C. Pang Cheng-MinTI-Development of a Novel Transparent Flexible Capacitive Micromachined Ultrasonic Transducer, *Sensors* **2017**, *17*
[7] N. A. Kyeremateng, T. Brousse, D. Pech, *Nature Nanotechnology* **2017**, *12*, 7–15.
[8] Z.-S. Wu, X. Feng, H.-M. Cheng, *National Science Review* **2014**, *1*, 277–292.
[9] M. Beidaghi, Y. Gogotsi, *Energy Environ. Sci.* **2014**, *7*, 867–884.
[10] A. Soam, N. Arya, A. Singh, R. Dusane, *Chemical Physics Letters* **2017**, *678*, 46–50.
[11] J. P. Alper, M. Vincent, C. Carraro, R. Maboudian, *Appl. Phys. Lett.* **2012**, *100*, 163901.
[12] J. P. Alper, S. Wang, F. Rossi, G. Salviati, N. Yiu, C. Carraro, R. Maboudian, *Nano Lett.* **2014**, *14*, 1843–1847.
[13] F. Thissandier, N. Pauc, T. Brousse, P. Gentile, S. Sadki, *Nanoscale Research Letters* **2013**, *8*, 38.
[14] F. Thissandier, A. Le Comte, O. Crosnier, P. Gentile, G. Bidan, E. Hadji, T. Brousse, S. Sadki, *Electrochemistry Communications* **2012**, *25*, 109–111.
[15] D. Aradilla, P. Gentile, G. Bidan, V. Ruiz, P. Gómez-Romero, T. J. S. Schubert, H. Sahin, E. Frackowiak, S. Sadki, *Nano Energy* **2014**, *9*, 273–281.
[16] D. Wei, S. J. Wakeham, T. W. Ng, M. J. Thwaites, H. Brown, P. Beecher, *Electrochemistry Communications* **2009**, *11*, 2285–2287.
[17] M. Brachet, D. Gaboriau, P. Gentile, S. Fantini, G. Bidan, S. Sadki, T. Brousse, J. Le Bideau, *J. Mater. Chem. A* **2016**, *4*, 11835–11843.
[18] Y. Bencheikh, M. Harnois, R. Jijie, A. Addad, P. Roussel, S. Szunerits, T. Hadjersi, S. El Hak Abaidia, R. Boukherroub, *Electrochimica Acta* **2019**, *311*, 150–159.
[19] W. Zheng, Q. Cheng, D. Wang, C. V. Thompson, *Journal of Power Sources* **2017**, *341*, 1–10.
[20] B. Asbani, B. Bounor, K. Robert, C. Douard, L. Athouël, C. Lethien, J. Le Bideau, T. Brousse, *Journal of The Electrochemical Society* **2020**, *167*, 100551.
[21] A. Kisliuk, V. Bocharova, I. Popov, C. Gainaru, A. P. Sokolov, *Electrochimica Acta* **2019**, *299*, 191–196.
[22] V. Bocharova, Z. Wojnarowska, P.-F. Cao, Y. Fu, R. Kumar, B. Li, V. N. Novikov, S. Zhao, A. Kisliuk, T. Saito, J. W. Mays, B. G. Sumpter, A. P. Sokolov, *J. Phys. Chem. B* **2017**, *121*, 11511–11519.
[23] J. R. Deka, D. Saikia, G.-W. Lou, C.-H. Lin, J. Fang, Y.-C. Yang, H.-M. Kao, *Materials Research Bulletin* **2019**, *109*, 72–81.
[24] R. S. Assary, L. A. Curtiss, P. C. Redfern, Z. Zhang, K. Amine, *J. Phys. Chem. C* **2011**, *115*, 12216–12223.
[25] A. K. Bharwal, N. A. Nguyen, C. Iojoiu, C. Henrist, F. Alloin, *Solid State Ionics* **2017**, *307*, 6–13.
[26] Z. Zhu, A. G. Einset, C.-Y. Yang, W.-X. Chen, G. E. Wnek, *Macromolecules* **1994**, *27*, 4076–4079.

[27] Z. Zhang, L. J. Lyons, R. West, K. Amine, R. West, *Silicon Chemistry* **2007**, *3*, 259–266.
[28] Y. Kang, J. Lee, D. H. Suh, C. Lee, *Journal of Power Sources* **2005**, *146*, 391–396.
[29] J.-J. Kang, W.-Y. Li, Y. Lin, X.-P. Li, X.-R. Xiao, S.-B. Fang, *Polymers for Advanced Technologies* **2004**, *15*, 61–64.
[30] Z. Hou, C. Kan, *Journal of Surfactants and Detergents* **2015**, *18*, 517–522.
[31] R. Rohan, K. Pareek, Z. Chen, W. Cai, Y. Zhang, G. Xu, Z. Gao, H. Cheng, *J. Mater. Chem. A* **2015**, *3*, 20267–20276.
[32] X. Zhan, J. Zhang, M. Liu, J. Lu, Q. Zhang, F. Chen, *ACS Appl. Energy Mater.* **2019**, *2*, 1685–1694.
[33] S. Kalybekkyzy, A.-F. Kopzhassar, M. V. Kahraman, A. Mentbayeva, Z. Bakenov, *Polymers* **2021**, *13*
[34] J.-H. Hong, J. W. Kim, S. Kumar, B. Kim, J. Jang, H.-J. Kim, J. Lee, J.-S. Lee, *Journal of Power Sources* **2020**, *450*, 227690.
[35] H.-P. Liang, M. Zarrabeitia, Z. Chen, S. Jovanovic, S. Merz, J. Granwehr, S. Passerini, D. Bresser, *Advanced Energy Materials* **2022**, *12*, 2200013.
[36] A. K. Bharwal, L. Manceriu, C. Iojoiu, J. Dewalque, T. Toupance, L. Hirsch, C. Henrist, F. Alloin, *ACS Appl. Energy Mater.* **2018**, *1*, 4106–4114.
[37] A. K. Bharwal, G. D. Salian, L. Manceriu, A. Mahmoud, F. Alloin, C. Iojoiu, T. Djenizian, C. M. Ruiz, M. Pasquinelli, T. Toupance, C. Olivier, D. Duché, J.-J. Simon, C. Henrist, *Applied Surface Science Advances* **2021**, *5*, 100120.
[38] M. P. Cipolla, G. L. De Gregorio, R. Grisorio, R. Giannuzzi, G. Gigli, G. P. Suranna, M. Manca, *Journal of Power Sources* **2017**, *356*, 191–199.
[39] G. L. De Gregorio, R. Giannuzzi, M. P. Cipolla, R. Agosta, R. Grisorio, A. Capodilupo, G. P. Suranna, G. Gigli, M. Manca, *Chem. Commun.* **2014**, *50*, 13904–13906.
[40] M. T. Tsehaye, N. H. Choi, P. Fischer, J. Tübke, E. Planes, F. Alloin, C. Iojoiu, *ACS Appl. Energy Mater.* **2022**, *5*, 7069–7080.
[41] D. Gaboriau, M. Boniface, A. Valero, D. Aldakov, T. Brousse, P. Gentile, S. Sadki, *ACS Appl. Mater. Interfaces* **2017**, *9*, 13761–13769.
[42] A. Valero, A. Mery, D. Gaboriau, M. Dietrich, M. Fox, J. Chretien, N. Pauc b, P.Y. Jouan, P.l Gentile, S. Sadki, Electrochimica Acta. 2021, 389, 1, 138727
[43] N. De Vos, C. Maton, C. V. Stevens, *ChemElectroChem* **2014**, *1*, 1258–1270.
[44] M. P. S. Mousavi, S. Kashefolgheta, A. Stein, P. Bühlmann, *Journal of The Electrochemical Society* **2015**, *163*, H74–H80.
[45] P. C. Howlett, E. I. Izgorodina, M. Forsyth, D. R. MacFarlane, **2006**, *220*, 1483–1498.
[46] V. R. Koch, L. A. Dominey, C. Nanjundiah, M. J. Ondrechen, *Journal of The Electrochemical Society* **1996**, *143*, 798.
[47] M. Ue, A. Murakami, S. Nakamura, *Journal of The Electrochemical Society* **2002**, *149*, A1572.

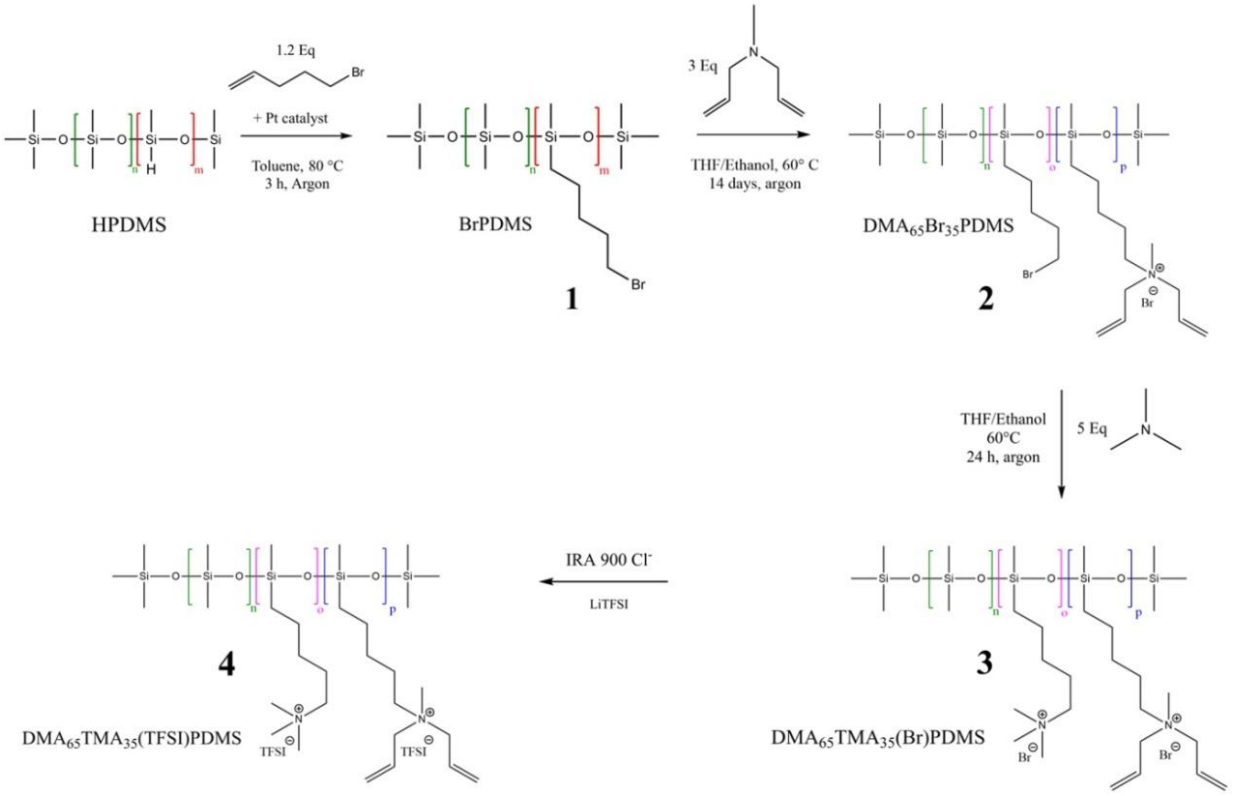

Figure 1. Synthesis process of the polymer electrolyte: 1) Hydrosililation reaction, 2) Quaternization of diallylmethylamine, 3) Quaternization of trimethylamine 4) Anion exchange from bromide to bis(trifluorosulfonyl)imide anion.

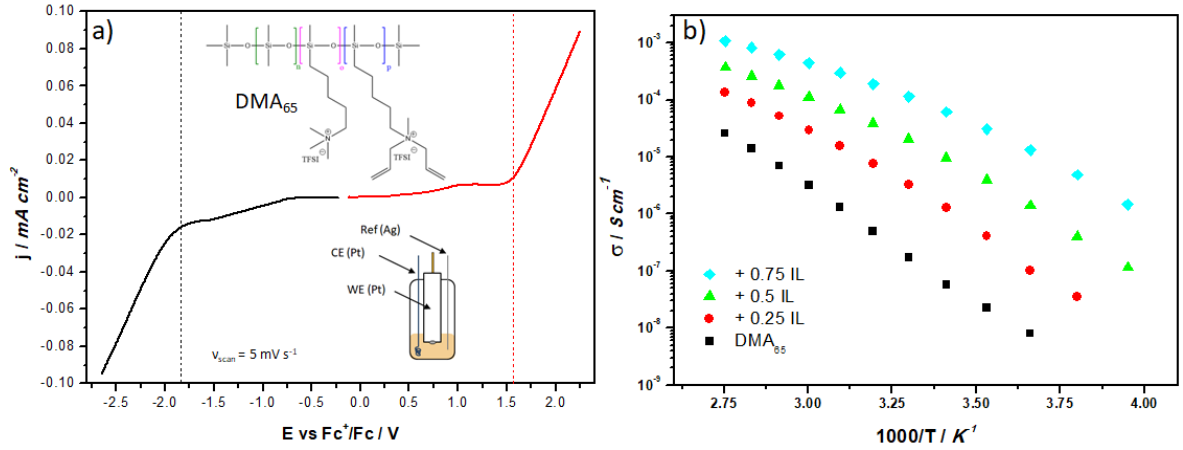

Figure 2. Electrochemical characterization of $DMA_{65}TMA_{35}(TFSI)PDMS$ a) electrochemical stability in 3 electrodes system composed by a Pt working electrode, a Pt counter electrode and a silver rod as reference. In red the oxidation part and in black the reduction part. v_{scan} = 5 mV s^{-1} b) conductivity of membrane with different composition. Darocur 1173 is used as UV initiator for each membrane. In black the crosslinked membrane is composed of $DMA_{65}TMA_{35}(TFSI)PDMS$, in red with an addition of 0.25 molar equivalent of IL with regards to ammonium moieties in the polymer, in green 0.5 molar equivalent and in cyan, 0.75 molar equivalent.

Table 1. Conductivity at 0, 20 and 90 °C and T_g of the crosslinked membranes

	$DMA_{65}TMA_{35}$(TFSI)PDMS	+ 0.25 IL	+ 0.50 IL	+ 0.75 IL
$\sigma_{0°C}$ (S/cm)	7.9 10^{-9}	1.0 10^{-7}	1.4 10^{-6}	1.3 10^{-5}
$\sigma_{20°C}$ (S/cm)	5.7 10^{-8}	1.3 10^{-6}	9.6 10^{-6}	6.2 10^{-5}
$\sigma_{90°C}$ (S/cm)	2.6 10^{-5}	1.4 10^{-4}	3.710^{-4}	1.1 10^{-3}
T_g /°C	-49	-69	-73	-75

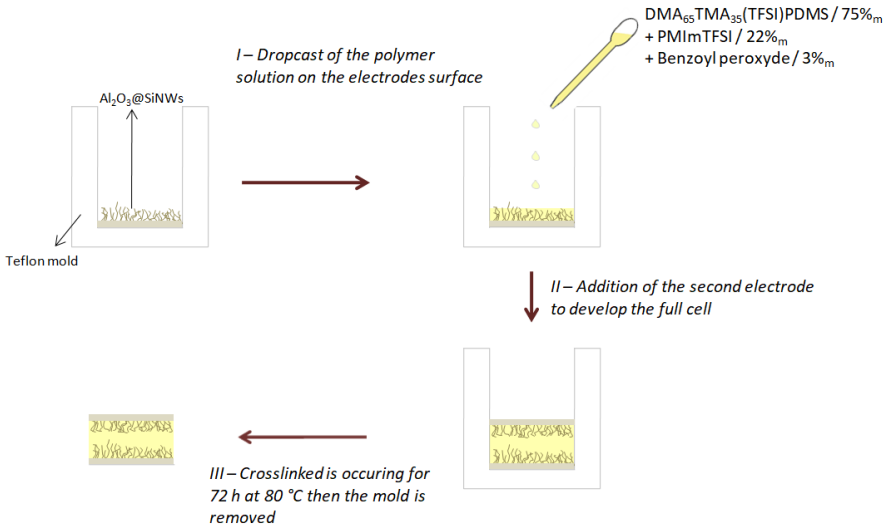

Scheme 1. Preparation process of the full cell device with $DMA_{65}TMA_{35}$(TFSI)PDMS + 0.5 IL

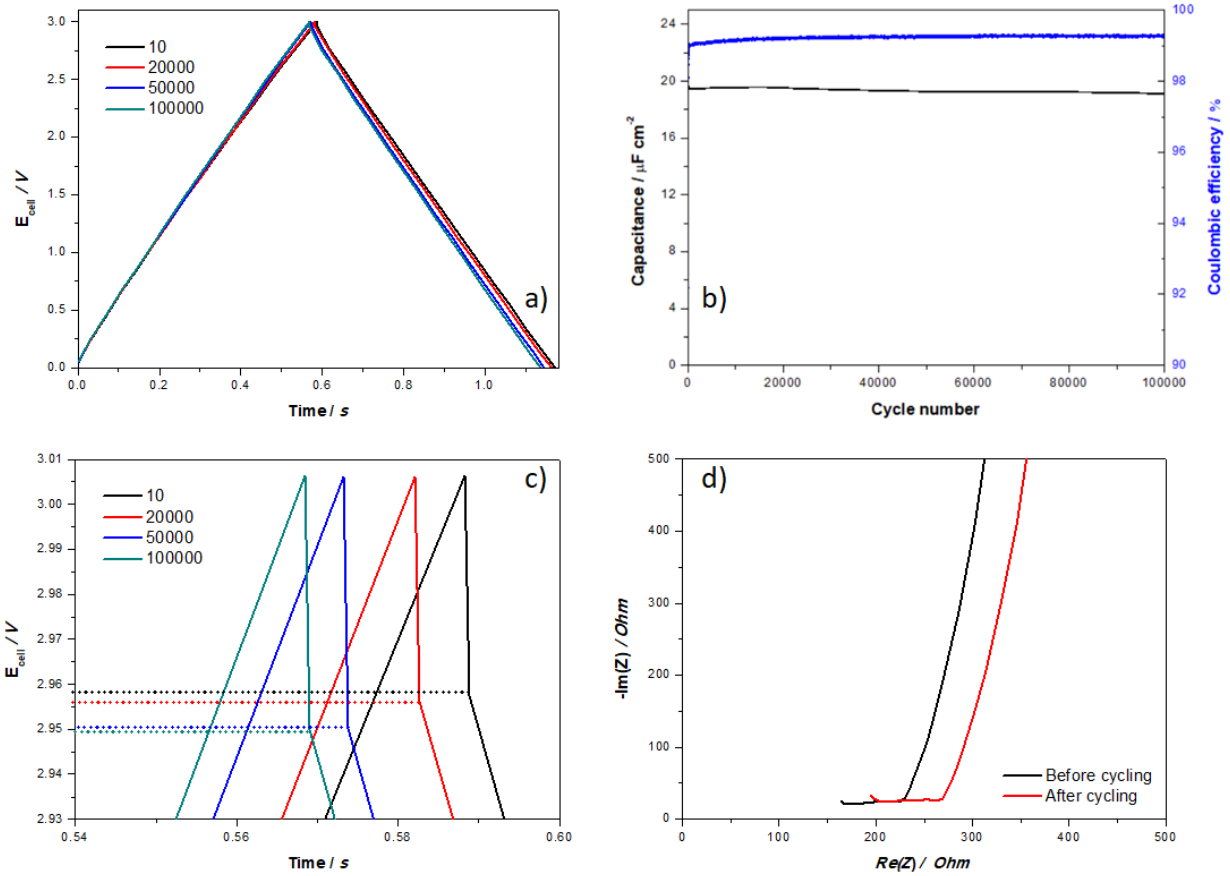

Figure 3. Cycling stability of the symetric device using Al_2O_3@SiNWs electrodes and crosslinked electrolyte containing $DMA_{65}TMA_{35}$(TFSI)PDMS + 0.50 IL over a 100 000 galvanostatic charge/discharge study. a) Galvanostatic measurement of the device. Cycles 10, 20 000, 50 000 and 100 000 are represented. b) Capacitance and coulombic efficiency of the device upon cycling. c) Evolution of the ohmic drop during galvanostatic cycling. d) Nyquist plot of the symetric device before and after cycling.

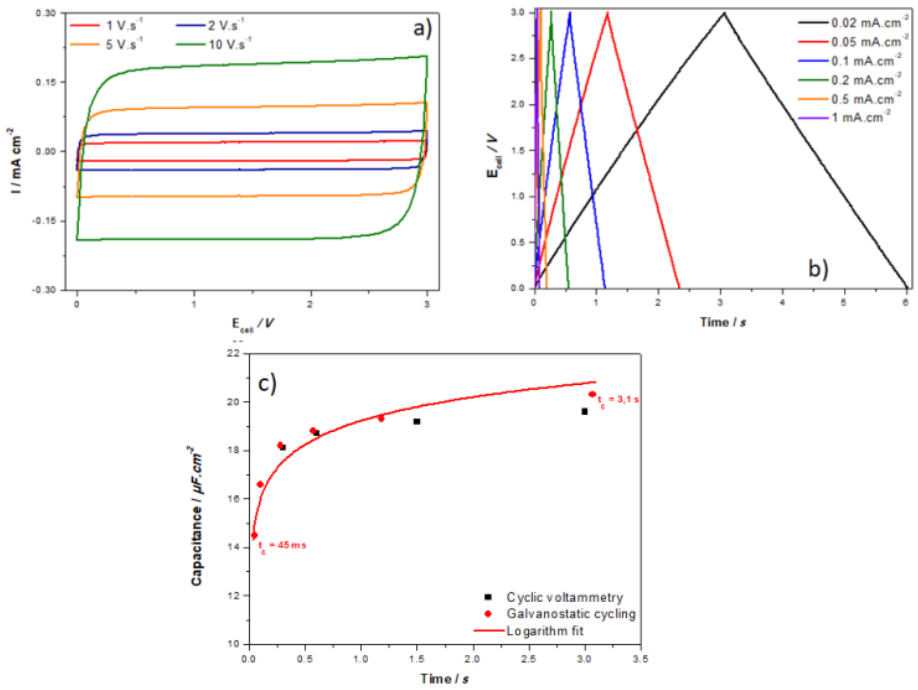

Figure 4. Impact of the charging time on the device performances. a) Cyclic voltammetry of the full cell for different scan rates. b) Galvanostatic cycling of the full cell for different current densities.c) Capacitance of the device with regards to charge time

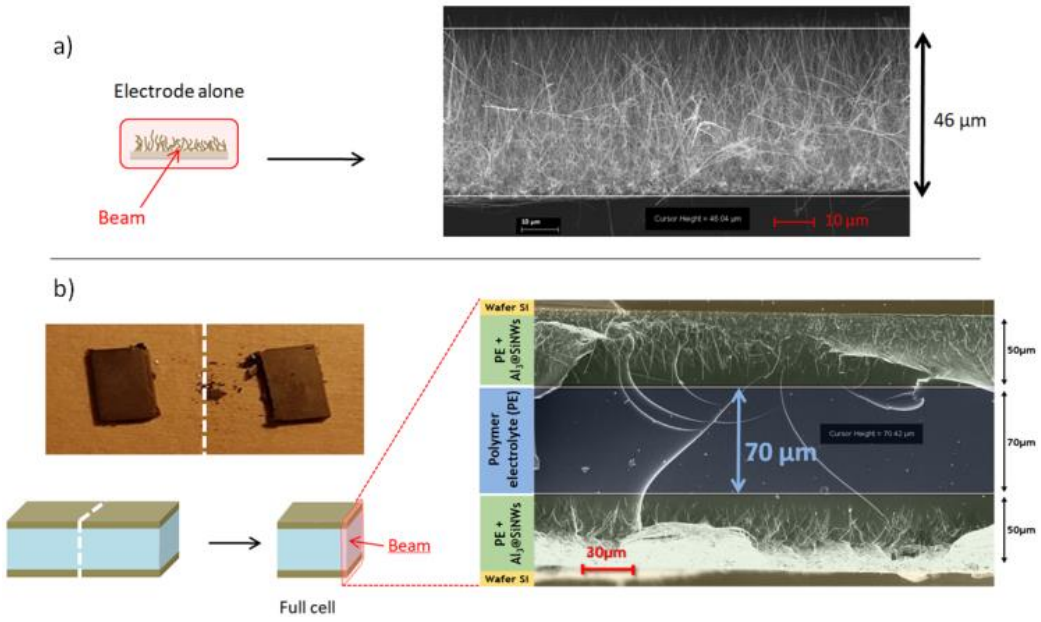

Figure 5. SEM Images of a) the Al_2O_3@SiNWs electrode b) the slice of the full cell device that was clived in half

All the figures presented needs to be colored on printed version.